

# High-efficiency ultrasmall polarization converter in InP membrane

Josselin Pello,<sup>1,\*</sup> Jos van der Tol,<sup>1</sup> Shahram Keyvaninia,<sup>2</sup> René van Veldhoven,<sup>1</sup>  
Huub Ambrosius,<sup>1</sup> Gunther Roelkens,<sup>2</sup> and Meint Smit<sup>1</sup>

<sup>1</sup>COBRA Research Institute, Eindhoven University of Technology, P.O. Box 513, Eindhoven 5600 MB, The Netherlands

<sup>2</sup>Photonic Research Group, INTEC, Ghent University-IMEC, Sint-Pietersnieuwstraat 41, Ghent 9000, Belgium

\*Corresponding author: [josselin.pello@gmail.com](mailto:josselin.pello@gmail.com)

Received June 1, 2012; revised July 19, 2012; accepted July 19, 2012;

posted July 20, 2012 (Doc. ID 169686); published August 31, 2012

An ultrasmall ( $<10 \mu\text{m}$  length) polarization converter in InP membrane is fabricated and characterized. The device relies on the beating between the two eigenmodes of chemically etched triangular waveguides. Measurements show a very high polarization conversion efficiency of  $>99\%$  with insertion losses of  $<-1.2 \text{ dB}$  at a wavelength of  $1.53 \mu\text{m}$ . Furthermore, our design is found to be broadband and tolerant to dimension variations. © 2012 Optical Society of America

OCIS codes: 130.3120, 130.5440, 230.7370.

Polarization handling is a fundamental issue in photonic integrated circuits. Since the propagation properties of the TE and TM polarized modes often differ strongly, most devices only function well for a single polarization. A polarization diversity scheme is then required in order to process the orthogonally polarized light [1]. Besides, polarization can in some cases be taken advantage of, e.g., for light intensity modulation or polarization bit interleaving [2]. For all these applications, an efficient broadband polarization converter is the key component.

Recently, several polarization rotators with conversion lengths below  $<50 \mu\text{m}$  have been demonstrated, mostly on the silicon-on-insulator (SOI) platform. The shortest ones ( $\sim 10 \mu\text{m}$ ) are based on L-shaped cross-section waveguides [3], or waveguides with two subwavelength trenches of different depths [4]. However, these two designs both rely on relatively tight fabrication accuracies (alignment between two etching steps for the former, and nanometer-resolution lithography for the latter). A more tolerant device based on the cross-polarization coupling effect has shown good performance [5], but at the price of a longer conversion length ( $44 \mu\text{m}$ ). Finally, an ultrashort ( $2 \mu\text{m}$  long) polarization converter design based on a triangular waveguide etched at  $45^\circ$  was proposed in [6], showing very good simulated performance, but with a high sensitivity to the etching angle.

In this Letter, we report on the fabrication and characterization of a polarization converter similarly based on triangular waveguides for a short device, but optimized for high tolerance to fabrication errors [7]. This high tolerance is obtained by the use of wet etching to create  $35^\circ$  triangular waveguides with crystallographic accuracy, and by the minimization of the conversion length during the design (which sets the operation point of the device at a local minimum). It is, to our knowledge, the smallest polarization converter ever made in InP ( $0.4 \times 0.8 \times 7.5 \mu\text{m}^3$ ). Measurements show very high TE-to-TM polarization conversion efficiency (PCE) ( $>99\%$ ) and low-loss operation ( $<-1.2 \text{ dB}$ ) at a wavelength of  $1.53 \mu\text{m}$ , while the conversion remains higher than  $92\%$  over a  $35 \text{ nm}$  wavelength range. These performances are similar to the state-of-the-art rotators made to date on SOI [3–5].

The diagram of the presented polarization converter is shown in Fig. 1. The device is composed of two oppositely loaded triangular waveguides with a rectangular waveguide section in between. Due to their geometry, triangular cross-section waveguides sustain eigenmodes  $E_1$  and  $E_2$  that are tilted with respect to the usual TE and TM polarization orientation. As a result, the TE or TM polarization state of the light entering the device is projected onto these eigenmodes, and both  $E_1$  and  $E_2$  are excited. Furthermore, the strong asymmetry inherent to triangular waveguides makes them highly birefringent (i.e., the difference in propagation constants between  $E_1$  and  $E_2$  is relatively high). This means that  $E_1$  and  $E_2$  will beat (and effectively rotate the polarization state of the light) over a rather short propagation distance. As shown in [7], two oppositely loaded triangular waveguides are required for full TE to TM conversion, because the angle between the  $(E_1, E_2)$  and  $(\text{TE}, \text{TM})$  systems in the considered wet-etched triangular waveguides is not  $45^\circ$ , but closer to  $23^\circ$ .

A detailed analysis of the design of the triangular section lengths can be found in [7], together with a discussion on the device's sensitivity to the height  $h$  of the triangular waveguides. In this Letter, the dimensions were chosen as  $h = 400 \text{ nm}$  and  $L_{\text{tri}} = 2.35 \mu\text{m}$  for both triangular sections. The rectangular waveguide between the two triangular sections was added for characterization purposes (as will be explained below).

The presented polarization converter is first fabricated using standard lithography, dry-etching, and wet-etching steps on a III-V epitaxial layer-stack. It is then bonded on a carrier wafer and released from the initial substrate by

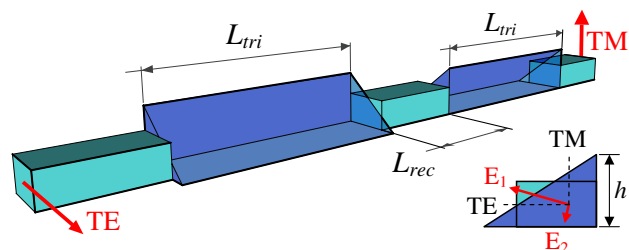


Fig. 1. (Color online) Diagram of the polarization converter, and (Inset) depiction of the triangular waveguide eigenmodes.

selective wet-etch. As shown in Fig. 2(a)i, the layers grown by MOVPE on the InP substrate before fabrication can be separated into a stack (1) (InGaAs-100 nm/InP-200 nm/InGaAs-100 nm), which is used to protect the membrane during substrate removal, and a stack (2) (InP-250 nm/InGaAsP-20 nm/InP-130 nm), which forms the membrane and will contain the devices. The 20 nm-thin InGaAsP layer in the membrane is used to define very accurately two different membrane thicknesses, with minimum damage to the material. After depositing a 50 nm-thick SiN<sub>x</sub> layer on the sample by plasma-enhanced chemical vapor deposition (PECVD), an e-beam lithography step, with ZEP520 resist, is used to open the nitride in the areas where the membrane should be only 250 nm-thick (e.g., for the input and output rectangular waveguides of the polarization converter). The sample is then etched chemically first in a solution (A) 1HCl:4H<sub>3</sub>PO<sub>4</sub> and subsequently in a solution (B) 1H<sub>2</sub>SO<sub>4</sub>:1H<sub>2</sub>O<sub>2</sub>:10H<sub>2</sub>O, to selectively remove the (InP-130 nm/InGaAsP-20 nm) layers from the areas opened in the nitride [see Fig. 2(a)ii].

In the following step, the rectangular waveguides and the vertical sidewalls of the triangular waveguides of the future polarization converter are defined simultaneously, using e-beam lithography on a new SiN<sub>x</sub> layer. The pattern is then transferred to the III-V layers using a CH<sub>4</sub>-H<sub>2</sub> reactive ion etching (RIE) process [cf. Fig. 2(a)iii].

The last part of the polarization converters patterning consists in the fabrication of the sloped sidewalls of the triangular waveguides. A new 200 nm-thick SiN<sub>x</sub> layer is deposited, and a final e-beam lithography is used to open locally the areas of the future triangular waveguides [see Fig. 2(a)iv]. The SiN<sub>x</sub> layer is then etched in a CHF<sub>3</sub>-O<sub>2</sub> RIE process, controlling the etching time in such a way that the SiN<sub>x</sub> is removed from the horizontal areas but not from the vertical sidewalls defined previously. This is rendered possible by the good conformality of the

SiN<sub>x</sub> PECVD deposition and the strong verticality of the SiN<sub>x</sub> RIE process used. Finally, the stack (2) is etched chemically in the regions opened in the SiN<sub>x</sub> layer, using the solutions (A) and (B) mentioned previously. Since the etching produced by these solutions stops on the (112) plane of InP, a 35° slope running from the top of the SiN<sub>x</sub> covered sidewall to the first InGaAs etch-stop layer below is obtained [see Fig. 2(b)].

After the triangular waveguides have been created, the SiN<sub>x</sub> layer is removed. The InP chip is then covered with a SiO<sub>2</sub> cladding for improved adhesion, and bonded upside-down on a silicon carrier wafer using a 50 nm-thick BCB (Benzo-cyclo-butene) layer. Finally, the substrate and the stack (1) are removed by wet-etch [cf. Fig. 2(a)vi].

Due to their high coupling efficiency and relative ease of fabrication, grating couplers are often used to couple light into and out of membrane photonics chips [3]. However, these diffractive structures are optimized for exciting a given mode in the chip, and in practice they suppress the orthogonally polarized light with a 50 dB extinction ratio. As a consequence, when grating couplers are used, it is not possible to directly measure the polarization state of the output light while rotating the input polarization. In order to measure the device's polarization conversion characteristics, while coupling only TE light in and out of the chip, we used an alternative technique, based on the variation of the length  $L_{\text{rec}}$  of the device's central rectangular section (cf. Fig. 1).

The design of the polarization converter was optimized for  $L_{\text{rec}} = 0 \mu\text{m}$  and  $L_{\text{tri}} = 2.35 \mu\text{m}$ . As described in [7], for a TE-polarized input light, the polarization state after propagating through the first triangular section is a complex superposition of the TE and TM modes. Since the TE and TM modes propagate at different speed in the rectangular waveguide, a phase-shift is created between them that linearly increases with  $L_{\text{rec}}$ . Understandably, this phase-shift will distinctly modify the designed behavior of the polarization converter, and cause the polarization state of the light leaving the device after propagating through the second triangular waveguide to contain a TE component, instead of the fully TM polarized state predicted by design. More precisely, when  $L_{\text{rec}}$  is an odd multiple of  $L_{\pi} = \pi/(\beta_{\text{TE}} - \beta_{\text{TM}})$  (where  $\beta_{\text{TE,TM}}$  are the propagation constants of the standard TE and TM modes), the conversion in the second triangular section is reversed w.r.t. the first one; therefore the output polarization state should be fully TE-polarized. Conversely, when  $L_{\text{rec}}$  is an even multiple of  $L_{\pi}$ , the polarization state is the same before and after the rectangular section, and the device again functions as a TE-to-TM polarization converter. As expected from the wave nature of light, the linear relation between the phase-shift created in the rectangular section and its length  $L_{\text{rec}}$  is translated into a (cosine)<sup>2</sup> variation of the TE-TE transmission versus  $L_{\text{rec}}$ .

Three sets of 16 devices each were fabricated. For each set, the length of the triangular waveguides was kept constant ( $L_{\text{tri}} = 2.1 \mu\text{m}$ ,  $2.35 \mu\text{m}$  and  $2.6 \mu\text{m}$ , respectively), while the length  $L_{\text{rec}}$  of the central rectangular waveguide was varied continuously (from 4 to 11.5  $\mu\text{m}$ ). The TE-TE transmission of each device at a wavelength of  $\lambda = 1.53 \mu\text{m}$  was measured separately using the setup of Fig. 3(a), and normalized to the average transmission

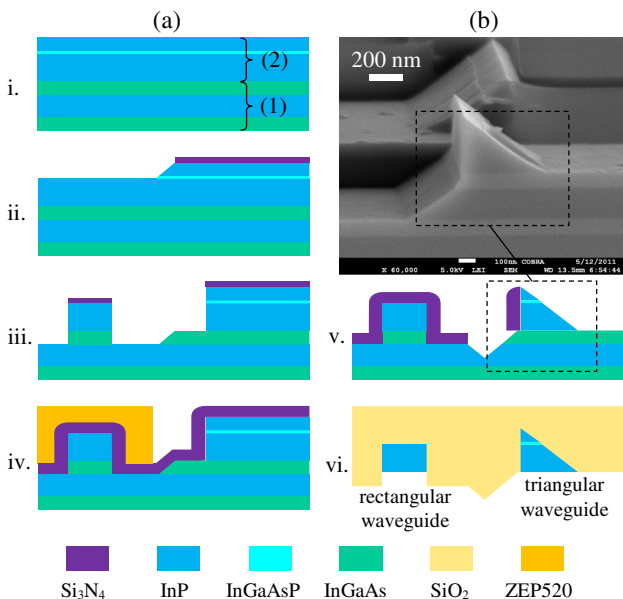


Fig. 2. (Color online) (a) Process-flow used to fabricate the polarization converter; (b) SEM picture of a fabricated device, corresponding to step v. of the process-flow in (a).

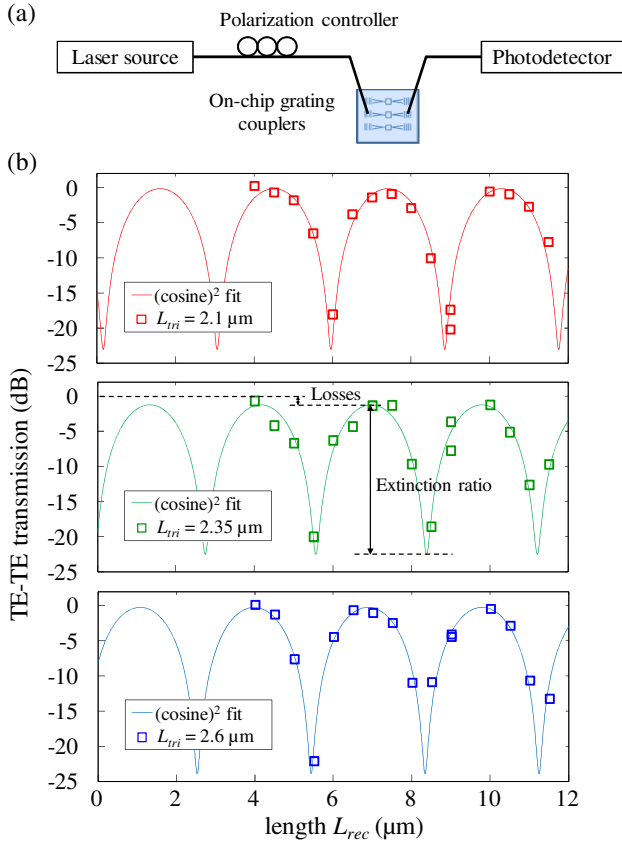


Fig. 3. (Color online) (a) Schematic of the setup used to characterize the devices; (b) Measured TE-TE transmission of the device of Fig. 1 at  $\lambda = 1.53 \mu\text{m}$ , as a function of the length  $L_{\text{rec}}$  of the central rectangular section. The three graphs correspond to three sets of devices (with  $L_{\text{tri}} = 2.1, 2.35,$  and  $2.6 \mu\text{m}$ ).

through a set of waveguides of identical length. The results are plotted as a function of  $L_{\text{rec}}$  in Fig. 3(b). Each set of data is fitted with a  $(\cos)^2$  function, which is then used to determine the insertion losses and PCE of each set's best possible device. The usual definition of the PCE,  $P_{\text{TM}}/(P_{\text{TE}} + P_{\text{TM}})$  at the device's output, is rewritten here as  $\text{PCE} = 1/(1 + 10^{\text{ER}/10})$ , with ER the extinction ratio of the  $(\cos)^2$  function.

For each of the three sets, we measure a maximum PCE of  $>99.2 \pm 0.2\%$  at  $\lambda = 1.53 \mu\text{m}$  ( $-\text{ER} > 21 \pm 1$  dB). Furthermore, the insertion losses for two sets ( $L_{\text{tri}} = 2.1$  and  $2.6 \mu\text{m}$ ) are found to be lower than  $< -0.2 \pm 1$  dB. The uncertainty in the values of both the insertion losses and the PCE is due to the variations ( $\pm 1$  dB) observed in the transmissions of the reference waveguides distributed over the chip. We attribute these variations to local nonuniformities in the BCB bonding layer thickness, which, while having no effect on the polarization conversion, is known to influence the efficiency of the grating couplers. As expected from the design [7], the point  $L_{\text{rec}} = 0 \mu\text{m}$  corresponds to a minimum in TE-TE transmission for the set  $L_{\text{tri}} = 2.35 \mu\text{m}$ . For the other two sets, the minimum is slightly shifted from  $L_{\text{rec}} = 0 \mu\text{m}$ , which means that the operation wavelength of the device will also be slightly shifted. Finally,

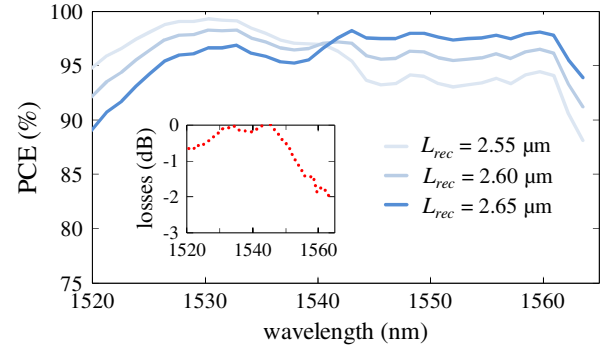


Fig. 4. (Color online) PCE and insertion losses (inset) as a function of wavelength for the device  $L_{\text{tri}} = 2.6 \mu\text{m}$  and  $L_{\text{rec}} = 2.6 \pm 0.05 \mu\text{m}$ .

although limited by the bandwidth of the grating couplers, the wavelength behavior of the three sets of devices was studied using a broadband superluminescent diode and an optical spectrum analyzer. The spectra of each set's 16 devices were recorded and then analyzed at each wavelength in the same way as in Fig. 3(b). The fitted  $(\cos)^2$  functions obtained for each wavelength give the insertion losses versus wavelength ( $\lambda$ ), and can be used to determine the TE-TE transmission spectrum of a device with any given  $L_{\text{rec}}$  value. The PCE is derived from the TE-TE transmission and plotted versus  $\lambda$  in Fig. 4, for  $L_{\text{tri}} = 2.6 \mu\text{m}$  and  $L_{\text{rec}} = 2.6 \pm 0.05 \mu\text{m}$ . This graph shows that for these parameters, the PCE is above  $>92\%$  and the losses below  $< -1.5 \pm 1$  dB over a wavelength range of 35 nm, with a  $\pm 50$  nm tolerance on  $L_{\text{rec}}$ .

In conclusion, we have demonstrated a polarization converter in InP membrane. The device is very short ( $< 10 \mu\text{m}$ , with less than  $< 5 \mu\text{m}$  possible without the central rectangular section) and efficient (PCE  $> 99\%$ , with losses  $< -1.2$  dB). Furthermore, it is broadband and tolerant to longitudinal dimension variations.

## References

1. H. Fukuda, K. Yamada, T. Tsuchizawa, T. Watanabe, H. Shinojima, and S. Itabashi, *Opt. Express* **16**, 4872 (2008).
2. P. Cho and J. Khurgin, *J. Opt. Netw.* **2**, 112 (2003).
3. D. Vermeulen, S. Selvaraja, W. Bogaerts, and G. Roelkens, "High-efficiency broadband CMOS-compatible polarization rotator on SOI," presented at the 7th International Conference on Group IV Photonics, Beijing, China, September 2010, paper WC6.
4. A. Velasco, M. Calvo, P. Cheben, A. Ortega-Moñux, J. Schmid, C. Alonso Ramos, Í. Molina Fernandez, J. Lapointe, M. Vachon, S. Janz, and D. Xu, *Opt. Lett.* **37**, 365 (2012).
5. L. Liu, Y. Ding, K. Yvind, and J. Hvam, *Opt. Lett.* **36**, 1059 (2011).
6. J. Yamauchi, M. Yamanoue, and H. Nakano, *J. Lightwave Technol.* **26**, 1708 (2008).
7. J. Pello, J. van der Tol, G. Roelkens, H. Ambrosius, and M. Smit, "Design of a new ultra-small polarization converter in InGaAsP/InP membrane," presented at the 15th European Conference on Integrated Optics, Cambridge, UK, April 2010, paper WeB2.